Systems & Control Transactions

Original Research Article
Peer Reviewed Conference Proceeding
ESCAPE 36 - European Symposium on Computer Aided Process Engineering
Sheffield, UK. 21-24 June 2026

PSE PRESS

Dynamic Modelling of Renewable-driven CO_2 Methanation using Recurrent Neural Networks

M. Andrea Pappagallo[ab], Diego A. Romero Lombo[c], Mattia Vallerio[c], Emanuele Moioli[ac]*

[a] Paul Scherrer Institut, Center for Energy and Environmental Sciences, Villigen, Switzerland
[b] École Polytechnique Fédérale de Lausanne, Institute of Chemical Science and Engineering, Lausanne, Switzerland
[c] Politecnico di Milano, Dipartimento di Chimica, Materiali e Ingegneria Chimica 'Giulio Natta', Milano Italy
* Corresponding Author: emanuele.moioli@polimi.it.

ABSTRACT

A recurrent neural network (RNN) model for a CO_2 methanation reactor was developed based on synthetic data generated from a validated mechanistic model of the same unit. The model was used to predict the main properties of the reactor – methane productivity and hotspot temperature – during a dynamic operation of the unit. The dynamic profile of feedstock availability was simulated taking into account the H_2 flow that can be produced from PV-powered water electrolysis using solar irradiation profiles over a year in Milan, Italy. The dataset therefore consists of 366 data instances (one for each day), each composed of one datapoint per minute of sunlight. The best agreement between the predictions from the RNN and the target output values from the mechanistic model was found using a shallow RNN of 20 hidden-layer neurons, trained with a batch size of 10 and an 80/20 training-testing split. This showed that RNNs can constitute a reliable tool for dynamic surrogate modelling of energy conversion reactors. The surrogate model was embedded in an energy system model to provide dynamic predictions of the energy conversion efficiency in the reactor, providing a more realistic performance assessment compared to the average efficiency models commonly used in the literature.

Keywords: Dynamic surrogate modelling, Recurrent neural networks, Machine learning, Energy systems analysis, Chemical reaction engineering

INTRODUCTION

The global transition towards decarbonised energy systems is reshaping the design and operation of chemical reactors within integrated energy networks. As renewable technologies become central to energy production, their inherent intermittency introduces temporal fluctuations that destabilise the conventional steady-state operation of chemical processes [1]. This shift demands new modelling approaches capable of capturing transient dynamics to ensure process efficiency, stability, and safety under variable operating conditions.

Among the technologies driving decarbonisation, the catalytic methanation of carbon dioxide (CO_2) has gained relevance within Power-to-Gas (PtG) systems. This process converts renewable hydrogen and captured CO_2 into synthetic natural gas (SNG), which can be injected into existing gas grids or used as a carbon-neutral fuel [2]. By enabling renewable energy storage and carbon utilisation, CO_2 methanation provides a key link between the renewable power and gas sectors. However, the highly exothermic nature of the reaction ($\Delta H_{298K} = -165.0 \frac{kJ}{mol}$) poses challenges for heat management and reactor stability, particularly under the intermittent and variable conditions imposed by renewable power fluctuations [3]. These dynamic changes in feed composition, flowrate, and temperature cannot be reliably represented through steady-state modelling approaches.

In this context, dynamic reactor modelling has emerged as a critical tool for understanding and optimising CO_2 methanation under varying conditions. By explicitly accounting for temporal variations in system inputs, dynamic modelling enables the prediction of phenomena such as transient temperature evolution, heat accumulation, and reaction rate fluctuations, providing the founda-

tion for safe and efficient reactor operation in non-stationary regimes [4]. Nevertheless, traditional mechanistic models, despite their physical accuracy, are computationally demanding due to the need to solve complex coupled differential equations across multiple spatial and temporal scales.

To overcome these limitations, recent advances in machine learning have opened new pathways for developing data-driven models that replicate mechanistic behaviour with significantly lower computational cost [5]. Recurrent neural networks (RNNs), in particular, have demonstrated great potential for modelling sequential and time-dependent chemical processes by capturing the effect of dynamic inputs on dynamically operated reactors [6].

This study develops and applies an RNN model trained on data from a validated mechanistic simulation to reproduce the dynamic behaviour of a CO_2 methanation reactor fed with hydrogen produced via photovoltaic-powered electrolysis. The main objective is to quantify the impact of seasonal renewable fluctuations on reactor performance and stability, providing a computationally efficient modelling framework to support future Power-to-Gas technologies.

While the tool of RNNs has been used in the literature to construct hybrid, discrepancy-based models [6, 7], i.e., dynamic mechanistic models where the machine learning tool is used to bridge the gap between the first-principles equations and the real-life phenomenon, this work aims at using the machine learning tool to construct a fully black-box model for the dynamic calculation of key performance variables in a chemical reactor as a function of present and past values of one or more selected input variables. This with the aim to realise a model as efficient as possible for the design of an energy conversion reactor capable of dealing with non-constant input quantities.

METHODS

The methodology adopted in this study consists of three main steps. First, a mechanistic reactor model was developed and validated to generate a synthetic dataset to support the machine learning model development. Subsequently, a surrogate dynamic model based on recurrent neural networks was designed and trained using this dataset. Finally, the model outputs were integrated into a black-box CO_2 methanation model to assess the dynamic behaviour of a PtG system and evaluate the performance and applicability of the predicted results.

Mechanistic reactor modelling

The kinetic expression for the CO_2 methanation reaction is derived from the work of Pétremand *et al.* (2025) [8]. Additionally, the behaviour of the system around the thermodynamic equilibrium is characterised by adding two kinetic expressions for the methanation of CO and the water-gas shift reaction from the work of Xu and Froment (1989) [9]. The rates of these reactions are only significant when the composition of the system is slightly different from that at the thermodynamic equilibrium, but not enough for the rate of CO_2 methanation to bridge such gap on its own. For the rest of the integration, their influence is negligible.

Table 1: Reactions in the kinetic model for CO methanation.

Reaction	Equation
CO_2 methanation	$CO_2 + 4H_2 \rightleftharpoons CH_4 + 3H_2O$
CO methanation	$CO + 3H_2 \rightleftharpoons CH_4 + 2H_2O$
Water-gas shift	$CO + H_2O \rightleftharpoons CO_2 + H_2$

The CO_2 methanation reactor considered in this study is a plate-type unit operating at 8 bar and thermally regulated with boiling water at 230 °C. The feed consists of biogas with a CO_2:CH4 ratio of 1:1, and hydrogen is supplied to achieve an inlet molar H_2/CO_2 ratio of 4. The dynamic behaviour of the reactor is represented using a one-dimensional dynamic model in which mass balances are pseudohomogeneous, while heat balances are heterogeneous.

The gas-phase component balance is expressed in Equation (1):

$$\frac{\partial F_i}{\partial t} + v_g \frac{\partial F_i}{\partial z} = v_g A \mathcal{D}_i \frac{\partial^2 c_i}{\partial z^2} + \rho_c (1-\varepsilon_b) v_g A \sum_{j=1}^{N_R} \nu_{ij} r_j \quad (1)$$

The energy balance equations for the gas and solid phases, respectively, are expressed in Equations (2) and (3):

$$\rho_g \hat{c}_{P_{mix}} \left(\frac{\partial T}{\partial t} + v_g \frac{\partial T}{\partial z}\right) = v_g A \frac{\partial}{\partial z}\left(\Lambda \frac{\partial T}{\partial z}\right) - v_g a_s h_s (T - T_s) - v_g a_e U (T - T_e) \quad (2)$$

$$(1-\varepsilon_b)\rho_s c_s \frac{\partial T_s}{\partial t} = -(1-\varepsilon_b)\rho_s \sum_{j=1}^{N_R} \Delta h_j^R r_j + v_g a_s h_s (T - T_s) \quad (3)$$

At the reactor inlet, the Danckwerts boundary conditions are applied, while zero-gradient Neumann conditions are imposed at the outlet by setting the second derivative of concentration and temperature to zero.

Hydrogen production from photovoltaic-powered electrolysis is determined using the efficiency η_{el} of the proton exchange membrane (PEM) electrolyser, defined as:

$$F_{H_2} = \frac{\eta_{el} W_{el}}{HHV_{H_2}} \quad (4)$$

In this formulation, the electrical power W_{el} corresponds to the installed photovoltaic capacity derived

from satellite observations for Milan, Italy, and an efficiency of 75% was assumed for the electrolyser.

Artificial neural network development

An artificial neural network (ANN) is a machine learning model that processes information through interconnected computational units known as neurons. Each neuron processes input signals (x), turning them into outputs (y) through two steps:

1. A linear combination of weights W and biases b;
2. A nonlinear activation function θ.

In the simplest ANN architecture, called a feed-forward neural network (FFNN), the neurons are organised in subsequent layers. The inputs to the network are processed by an input layer, one or more hidden layers, and one output layer [10].

The network parameters are initialised randomly, then updated iteratively to minimise the error between the actual and predicted outputs, in a procedure called training. Each iteration of the procedure is called epoch, and the training ends when a sufficient agreement between the training outputs and the network prediction is reached.

This study employs a recurrent neural network (RNN), which extends the conventional feedforward architecture by incorporating feedback connections to process sequential data and capture temporal dependencies relevant to reactor dynamics. A gated recurrent unit (GRU) network is used, as its gating mechanisms preserve information over longer time sequences through the hyperbolic tangent (tanh) and the sigmoid (σ) activation functions [11]. The GRU is defined by its gating mechanism, which at each time step k computes the reset gate $\boldsymbol{r}^{(k)}$, update gate $\boldsymbol{z}^{(k)}$, candidate gate $\boldsymbol{g}^{(k)}$, and the hidden state $\boldsymbol{h}^{(k)}$ (in the following equations, $\circ$ represents element-wise multiplication):

$$\boldsymbol{r}^{(k)} = \sigma\left(\boldsymbol{W}_r \boldsymbol{x}^{(k)} + \boldsymbol{R}_r \boldsymbol{h}^{(k-1)} + \boldsymbol{b}_r\right) \quad (5)$$

$$\boldsymbol{z}^{(k)} = \sigma\left(\boldsymbol{W}_z \boldsymbol{x}^{(k)} + \boldsymbol{R}_z \boldsymbol{h}^{(k-1)} + \boldsymbol{b}_z\right) \quad (6)$$

$$\boldsymbol{g}^{(k)} = \tanh\left(\boldsymbol{W}_g \boldsymbol{x}^{(k)} + \boldsymbol{r}^{(k)} \circ \left(\boldsymbol{R}_g \boldsymbol{h}^{(k-1)} + \boldsymbol{b}_g\right)\right) \quad (7)$$

$$\boldsymbol{h}^{(k)} = \left(\boldsymbol{1} - \boldsymbol{z}^{(k)}\right) \circ \boldsymbol{g}^{(k)} + \boldsymbol{z}^{(k)} \circ \boldsymbol{h}^{(k-1)} \quad (8)$$

Afterwards, the GRU hidden layer is linked to a fully connected output layer defined by its own weight vector and bias, yielding the network output $\boldsymbol{y}^{k}$:

$$\boldsymbol{y}^{(k)} = \boldsymbol{W}_y \boldsymbol{h}^{(k)} + \boldsymbol{b}_y \quad (9)$$

The RNN tool was used to produce a surrogate, data-driven model of the reactor where the only input feature is the hydrogen inlet flowrate, while the CO_2 is assumed to always be fed in stoichiometric amounts according to the Sabatier reaction (CO_2 methanation, Table 1). As output features, three performance variables for the methanation reactor were chosen in the hotspot temperature, the methane output flowrate, and the methane purity at the outlet.

As this study assesses a regression task, the predicted outputs are assessed against the target values using the mean squared error (MSE), which quantifies the average squared difference between the predictions y_i and target values $\hat{y}_i$:

$$\mathcal{L}_{MSE} = \frac{1}{N}\sum_{i=1}^{N}(y_i - \hat{y}_i)^2 \quad (10)$$

Integration into an energy system model

The trained RNN was integrated into a model for the design of a system to provide a constant supply of H_2 to satisfy the yearly energy demand from fuel-cell-powered vehicles. In this model, it is assumed that H_2 is primarily used in decarbonised mobility. When H_2 is available in excess, it is stored in the form of methane. Then, methane is reformed to produce hydrogen when H_2 supply is not sufficient [12] The energy demand is assumed as a problem datum and marked as W_{req}. The model equates W_{req} with the energy converted from solar to calculate the minimum PV panel surface required to meet the demand.

The energy from the PV panels is stored and converted according to three steps:

1. **electrolysis** to produce H_2,
2. **methanation** to convert the H_2 into CH_4,
3. **reforming** to reconvert the methane to hydrogen for use on vehicles.

Each of these steps is characterised by an efficiency value, resulting in the following equation for the conversion of the available energy W_{av}:

$$W_f = W_{av} \bullet \eta_{el} \bullet \eta_{meth} \bullet \eta_{ref} \quad (11)$$

While the efficiencies connected to the electrolysis and reforming steps are assumed constant ($\eta_{el} = 0.75, \eta_{ref} = 0.7$), the value of η_{meth} can either be a constant empirical value of 0.7, or calculated for each day individually with the help of the RNN model (in which case it is denoted by η_{RNN}):

$$\eta_{RNN} = \frac{F_{CH_4}^{out} \bullet HHV_{CH_4}}{F_{H_2}^{in} \bullet HHV_{H_2}} \quad (12)$$

The available energy for conversion is determined from the solar irradiation intensity I in the dataset:

$$W_{av} = I \bullet S_{PV} \quad (13)$$

The equivalence between W_{req} and W_f is then used to determine the required PV panel surface S_{PV}. Results are compared between the constant assumption of $\eta_{meth} = 0.7$ and the average of the daily values derived from the RNN model (η_{RNN}).

RESULTS AND DISCUSSION

Mechanistic reactor model validation

The mechanistic model was validated by reproducing the transient and steady-state behaviour of the reactor reported by Moioli *et al.* (2024) [13]. The transient thermal behaviour of the CO_2 methanation reactor was evaluated by analysing the temperature profiles every second minute during start-up. The modelling case used for the validation shown in Figure 1 has been obtained at a coolant temperature of 230°C, reactor pressure of 8 bar, and with an inlet composed of hydrogen and biogas in stoichiometric ratio, with the molar ratio of CO and CH_4 in the biogas assumed to be 1/1. The case in the figure refers to a step change in the inlet flowrate from 0% to 50% of the nominal design conditions of the reactor (3000 h^{-1}).

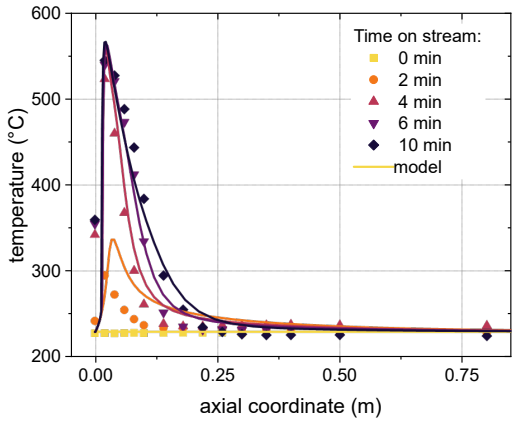

Figure 1: Temperature profile of the reactor during start-up at 50% load. Continuous lines represent the model results, scattered points the experimental data from [13].

At time-zero, the catalyst bed is preheated to 230°C. Upon feeding of CO_2, the reaction is initiated immediately, generating a hotspot whose axial width and peak temperature increase over time, reaching steady-state in under ten minutes. The mechanistic model successfully reproduces the start-up dynamics, closely matching the experimental observations. The discrepancies between the experimental and modelled profiles can be attributed to the difference between the catalysts used in the pilot-scale plant and in the work of Pétremand *et al.* [8].

The mechanistic model was subsequently validated through four simulations of the CO_2 methanation reactor, assessing its response to load variations, temperature evolution, concentration profiles, and axial temperature behaviour under different feed gas temperatures. In all cases, the reactor exhibited rapid thermal adaptation to changing operating conditions, and the model successfully reproduced key experimental reaction dynamics, including hotspot development and the attainment of grid-compliant methane. Overall, the simulated responses demonstrate the reliability and flexibility of the mechanistic model, confirming its suitability for generating representative training data.

RNN development and performance evaluation

The RNN was trained using three target variables: hotspot temperature, methane dry molar fraction, and methane molar flow. These descriptors were selected as key indicators because they represent the thermal behaviour of the reactor, product quality, and productivity under fluctuating hydrogen supply. To ensure balanced learning across variables of different magnitudes, a standardisation procedure that transforms all target variables into a comparable numerical range was applied:

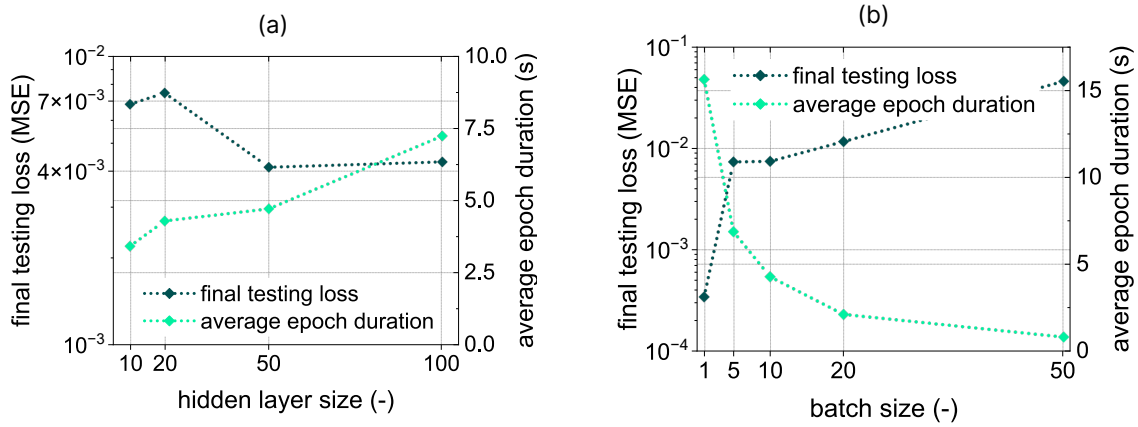

Figure 2: Effect of the number of neurons in the hidden layer (a) and of the training batch size (b) on the final performance of the RNN on the testing dataset – measured by mean squared error – and on the time required for the training.

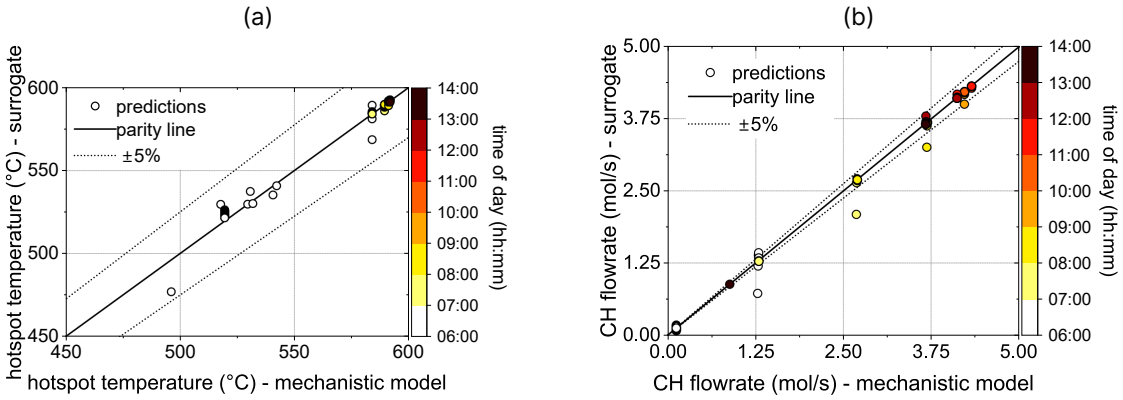

Figure 3: Parity plot for the hotspot temperature [°C] (a) and for the methane flowrate [mol/s] (b), comparing the values predicted by the RNN-based model (y axis) with those from the mechanistic model (x axis).

$$x_{i,sc} = \frac{(x_i - \mu_i)}{\sigma_i} \quad (14)$$

Where μ_i is the mean and σ_i the standard deviation of feature i across all datapoints. The scaling of the dataset allowed for stable convergence and close agreement between the predictions and the mechanistic model.

A sensitivity analysis was then performed to evaluate the influence of the hidden layer size, and batch size on model performance, whose results are reported in Figure 2. An increase in the hidden layer size did not lead to a clear improvement in the performance, but rather to a slight increase in the time needed for training. In machine learning theory, it is well established that increasing the number of neurons in hidden layers generally improves the accuracy of a neural network, but also that an excessive parametrisation may increase the risk of overfitting [6, 11]. The layer size for the following evaluations was therefore limited to 20 as a compromise to achieve relative accuracy while maintaining a low risk of overfitting and a manageable training time.

The sensitivity analysis on the batch size showed a clear trade-off between computational time and prediction accuracy: larger batch sizes reduced epoch duration but increased the testing loss. A batch size of 10 was adopted for the following evaluations, due to lower values also increasing the risk of overfitting.

The parity plots presented in Figure 3 offer an effective visual assessment of the model performance by comparing predicted values with their corresponding reference data for both output variables: the hotspot temperature, in °C, and the methane output of the reactor, in mol/s. Again, a strong agreement is shown between the predictions from the RNN model and those from the mechanistic model.

The parity plots show most data points lying close to the parity line, indicating that the RNN accurately reproduces the nonlinear behaviour of the mechanistic model under dynamic conditions. The highest deviations appear for the methane output at the extremes of the daytime range (lighter yellow datapoints), reflecting a reduced accuracy when the reactor operates at very low space velocities. These discrepancies remain limited and do not significantly affect overall predictive performance.

The parity plots confirm that the RNN captures both the steady-state and transient responses of the CO_2 methanation reactor with high fidelity.

Figure 4 compares the entire daily profile of the outlet flowrate of methane predicted by the mechanistic ground truth model and the RNN-based model, respectively. The strong agreement shown in the parity plot in Figure 2b between the predictions by the RNN and the mechanistic model is again made visible, confirming the ability of the network to capture the variation of key performance variables following a change in the hydrogen supply to the CO_2 methanation reactor.

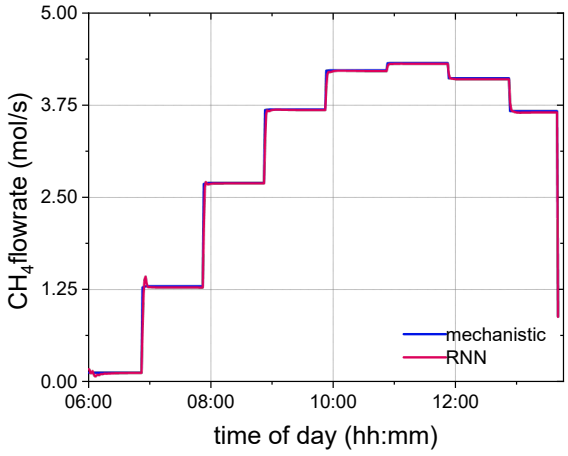

Figure 4: Comparison between the methane flowrate values [mol/s] predicted by the mechanistic model and the RNN-based model.

Table 2: Comparison of technical indicators obtained from the power-to-gas energy system using three modelling approaches.

	Constant efficiency	Average RNN efficiency
PV surface required $[\mathrm{m}^2]$	1001	989
Active days per year of the storage system $[\mathrm{d}]$	257	254
Required amount of energy carrier (CH_4) per year $[\mathrm{ton}]$	9.20	8.98
Required amount of biogas per year $\left[\frac{\mathrm{m}^3}{\mathrm{h}}\right]$	0.732	0.718

Integration into the energy system model

The recurrent neural network was integrated into the energy system model by applying the daily power-to-gas efficiency profile calculated in Equation (12). These daily efficiency values were incorporated into the macroscopic energy balance described in Equation (11), linking the dynamic reactor behaviour with the overall energy system evaluation. For comparison, the RNN results were assessed against those obtained using a constant efficiency value for the methanation block, as commonly done in energy system analysis [14]. The results are summarised in Table 2.

When comparing the constant efficiency evaluations with the ones conducted using a dynamic efficiency profile, some notable differences are found. First, the higher efficiencies calculated by the RNN model result in a 1.2% lower surface of PV panels needed to meet the energy demands, and a lower need for the energy storage system, which is used 3 days fewer than what calculated using the standard efficiency value.

This reduces the amount required over a year for both the energy carrier (-2.4%) and the biogas (-1.9%), leading to a more efficient use of resources.

These results show that integrating a dynamic efficiency profile, calculated with the help of a model, directly improves the energy balance and storage behaviour of the system model, whereas assuming constant efficiencies fails to capture the daily variations in performance. Including these variations provides a more realistic representation of the response of the PtG system to the intermittency typical of renewable energy sources.

CONCLUSIONS

This study developed and evaluated a recurrent neural network (RNN) framework for the dynamic modelling of a CO_2 methanation reactor powered by renewable hydrogen. The research aimed to bridge the gap between detailed mechanistic modelling, which provides high physical fidelity but is computationally intensive, and data-driven modelling, which enables fast, flexible, and adaptive simulations. The methodology consisted of three main stages: mechanistic model validation, RNN development, and a system evaluation within a Power-to-Gas (PtG) configuration.

In the first stage, a one-dimensional mechanistic reactor model using pseudohomogeneous component balances and heterogeneous energy balances was developed and validated with established CO_2 methanation kinetics. The model successfully reproduced the steady-state and transient responses reported in the literature [13], including the rapid thermal adaptation to load changes in the reactor, the evolution of the hotspot, and the corresponding concentration profiles. This validation confirmed the model as a reliable tool generating dynamic data representative of operating conditions influenced by fluctuating hydrogen inputs.

The second stage focused on developing and training the RNN using synthetic data produced by the mechanistic simulations. The hotspot temperature, methane dry molar fraction, and methane molar flow were selected to represent the thermal behaviour of the reactor, product quality, and productivity. Standardisation was essential to achieve balanced learning and stable convergence. A sensitivity analysis of network architecture showed that an increase in parametrisation (hidden layer size, network depth) had a limited influence on predictive accuracy, whereas the evaluation of the batch size revealed a clear trade-off between computational time and model performance. The final architecture, consisting of one hidden layer with 20 neurons and trained using a batch size of 10, provided the best balance between accuracy and efficiency. The trained RNN reproduced the nonlinear reactor dynamics with high fidelity, as demonstrated by strong agreement between predicted and mechanistic model outputs.

In the third stage, the RNN was integrated into a black-box PtG model to evaluate the system performance under daily and seasonal variability in hydrogen production from photovoltaic electrolysis. Compared to a constant efficiency assumption, the inclusion of dynamic daily efficiencies significantly altered the predicted behaviour of the chemical storage system. The dynamic case showed substantial decreases in the operating days needed to meet the energy demand, with a consequent decrease in the usage of methane and biogas, and in the PV panel surface required, demonstrating that simplified

efficiency assumptions notably overestimate the operational demands of the system.

Overall, this work demonstrates that RNNs offer an effective and computationally efficient surrogate for dynamic reactor modelling. The framework developed here constitutes a practical methodological approach that combines the accuracy of mechanistic models with the speed of data-driven ones, supporting future efforts in developing efficient optimisation and control strategies for flexible, renewable-driven chemical processes.

ACKNOWLEDGEMENTS

The authors acknowledge the support from the Swiss National Science Foundation (SNSF) Ambizione project: 'Moving catalyst vs. multi-catalyst: determination of the best reactor for the processing of unconventional feedstock' with grant number No. 20912.

TABLE OF VARIABLES

Mechanistic model

A	reactor cross-section	m^2
a_s	specific surface for interphase heat exchange	m^{-1}
c_i	concentration of species i	mol/m^3
$\hat{c}_{P_{mix}}$	mass-specific heat of gas mixture	$J/kg \cdot K$
c_s	specific heat of solids	$J/kg \cdot K$
$\mathcal{D}_i$	axial dispersion coefficient of species i	m^2/s
F_i	molar flowrate of component i	$kmol/s$
HHV_i	higher heating value of species i	J/mol
h_s	interphase heat exchange coefficient	$W/m^2 \cdot K$
$\dot{m}$	total mass flowrate	kg/s
r_j	rate of reaction j	$kmol/m^3 \cdot s$
T	temperature	K
T_e	coolant temperature	K
T_s	temperature of solid phase	K
t	time	s
U	global heat transfer coefficient	$W/m^2 \cdot K$
v_G	gas velocity	m/s
W_{el}	available electrical power	W
z	axial reactor coordinate	m
Δh_j^R	enthalpy of reaction j	J/mol
ε_b	bed void fraction	-
η_{el}	electrolyser efficiency	-
ν_{ij}	stoichiometric coefficient of species i in reaction j	-
ρ_C	catalyst density	kg/m^3

Surrogate model

$\boldsymbol{b}_g$	bias of gate g/output layer y
$\boldsymbol{g}^{(k)}$	candidate gate output at timestep k
$\boldsymbol{h}^{(k)}$	network hidden state at timestep k
$\boldsymbol{R}_g$	recurrent weights of gate g
$\boldsymbol{r}^{(k)}$	reset gate output at timestep k
$\tanh(\bullet)$	hyperbolic tangent activation function
$\boldsymbol{x}^{(k)}$	network input at timestep k
$\boldsymbol{y}^{(k)}$	network output at timestep k
$\boldsymbol{W}_g$	input weights of gate g/output layer y
$\boldsymbol{z}^{(k)}$	update gate output at timestep k
$\sigma(\bullet)$	sigmoid activation function

Energy system model

F_i^{in}	inlet flowrate of component i	$kmol/s$
F_i^{out}	outlet flowrate of component i	$kmol/s$
I	solar intensity	W/m^2
S_{PV}	total surface of PV panels	m^2
W_{av}	available power from PV plant	W
W_f	enthalpy content of final product	W
η_{el}	electrolyser efficiency	-
η_{meth}	thermal efficiency of methanation (constant hypothesis)	-
η_{RNN}	thermal efficiency of methanation (from surrogate model)	-

REFERENCES

1. Cegla M, Semrau R, Tamagnini F, Engell S. Flexible process operation for electrified chemical plants. Current Opinion in Chemical Engineering 39:100898 (2023). https://doi.org/10.1016/j.coche.2023.100898
2. Koschany F, Schlereth D, Hinrichsen O. On the kinetics of the methanation of carbon dioxide on coprecipitated nial(o). Applied Catalysis B: Environmental 181:504-516 (2016). https://doi.org/10.1016/j.apcatb.2015.07.026
3. Kreitz B, Wehinger GD, Turek T. Dynamic simulation of the CO2 methanation in a micro-structured fixed-bed reactor. Chemical Engineering Science 195:541-552 (2019). https://doi.org/10.1016/j.ces.2018.09.053
4. Tauer G, Kern C, Jess A. Transient effects during dynamic operation of a wall?cooled fixed?bed reactor for co₂methanation. Chem Eng & Technol 42:2401-2409 (2019). https://doi.org/10.1002/ceat.201900367
5. Schweidtmann AM, Esche E, Fischer A, Kloft M, Repke J, Sager S, Mitsos A. Machine learning in chemical engineering: a perspective. Chemie Ingenieur Technik 93:2029-2039 (2021).

https://doi.org/10.1002/cite.202100083
6. Wu Z, Rincon D, Christofides PD. Process structure-based recurrent neural network modeling for model predictive control of nonlinear processes. Journal of Process Control 89:74-84 (2020). https://doi.org/10.1016/j.jprocont.2020.03.013
7. Zhang D, del Río Chanona EA. Machine learning and hybrid modelling for reaction engineering. Royal Society of Chemistry (2023). https://doi.org/10.1039/9781837670178
8. Pétremand H, Witte J, Kröcher O, Moioli E. Machine learning-based kinetic modeling of the co₂ methanation reaction over an industrial catalyst. Ind. Eng. Chem. Res. 64:19864-19875 (2025). https://doi.org/10.1021/acs.iecr.5c02947
9. Xu J, Froment GF. Methane steam reforming, methanation and water-gas shift: I. Intrinsic kinetics. AIChE J 1989;35:88–96.
10. Yang L, Padding JT, Kuipers JAM. Two-fluid modelling for cylindrical fluidized beds using kinetic theory for rough spheres. Particuology 50:25-34 (2020). https://doi.org/10.1016/j.partic.2019.05.006
11. Zarzycki K, ?awry?czuk M. LSTM and GRU neural networks as models of dynamical processes used in predictive control: a comparison of models developed for two chemical reactors. Sensors 21:5625 (2021). https://doi.org/10.3390/s21165625
12. Madi H, Schildhauer T, Moioli E. Comprehensive analysis of renewable energy integration in decarbonised mobility: leveraging power-to-x storage with biogenic carbon sources. Energy Conversion and Management 321:119081 (2024). https://doi.org/10.1016/j.enconman.2024.119081
13. Moioli E, Senn P, Østrup S, Hütter C. Results from the operation of an efficient and flexible large-scale biogas methanation system. Energy Adv. 3:131-142 (2024). https://doi.org/10.1039/d3ya00436h
14. Elhaus N, Volkmann M, Kolb S, Schindhelm L, Herkendell K, Karl J. Techno-economic evaluation of anaerobic digestion and biological methanation in power-to-methane-systems. Energy Conversion and Management 315:118787 (2024). https://doi.org/10.1016/j.enconman.2024.118787